Modelling a Paraflex Loudspeaker System

Philipp Hovorka

BACHELOR'S THESIS

submitted to

Graz University of Technology

Supervisor

Dipl.-Ing. Dr.techn. Werner Weselak

Signal Processing and Speech Communication Laboratory

Head of Institute: Univ.-Prof. Dipl.-Ing. Dr.techn. Gernot Kubin

Graz, June 27, 2023

Abstract

In the past few years, development by the likes of M. Morgan J., D. Morgan and J. Vansickl for a new type of low frequency loudspeaker with high efficiency called "Paraflex" has brought up an alternative to the well established horn loaded or bass reflex loudspeaker designs for "Public Address" systems.
This new design is based on so called quarter wave resonators, which are highly related to acoustic transmission lines as used for "Transmission Line" loudspeaker systems. A lot of research has been made concerning this type of loudspeaker cabinet, dealing with wave propagation in acoustic tubes filled with absorbing materials and describing computational methods to deal with this kind of setup. However, the special configuration of a "Paraflex" loudspeaker with two transmission lines sitting at the front and back of the loudspeaker driver, merging close to the open end of the system, has not yet been reviewed.
This work therefore focuses on deriving a computational model for this kind of setup which yields the possibility of simulating most important system characteristics such as sound pressure output, phase response or electric impedance for a "Paraflex" loudspeaker cabinet. This is done by first making use of acoustic transmission line theory to obtain acoustic input impedance of the respective resonators. Subsequently, the electric analogous circuit of the system containing lumped elements only is analysed, which crucially makes it possible to compute membrane velocity as well as input sound pressure to the lines. Finally, output sound pressure can be obtained by again making use of acoustic transmission line theory. Simulation results of two specific setups will be discussed at the end of this work.

Bibliography

[1] M. M. J., *Paraflex: Public address loudspeaker enclosures*, https://www.facebook.com/groups/1657502687831078/permalink/3420769464837716, Accessed: 11-6-2023.

[2] R. A. Robinson, "An electroacoustic analysis of transmission line loudspeakers," Ph.D. dissertation, Georgia Institute of Technology, 2007.

[3] J. Backman, "A computational model of transmission line loudspeakers," in *Audio Engineering Society Convention 92*, Audio Engineering Society, 1992.

[4] M. Zollner and E. Zwicker, *Elektroakustik*. Springer-Verlag, 2013.

Contents

1 Introduction

"Public Address" loudspeaker design has always been focused on extending the low frequency response and increasing efficiency of loudspeaker cabinets to reduce power required for large venues while providing full range sound at an appropriate level.
This led to the development of various types of loudspeaker cabinets such as bass reflex systems for better low frequency response as well as horn loaded systems for increased efficiency.
However over the past few years, a new approach for high efficiency cabinets called "Paraflex" loudspeakers has come up, developed by its founders M. Morgan J., D. Morgan and J. Vansickle [1].
Like "Transmission Line" systems, this type of loudspeaker is based on quarter wave resonators, howbeit with a more complex geometric configuration.
Figure 1.1 b) shows the schematic of a "Paraflex" loudspeaker cabinet.

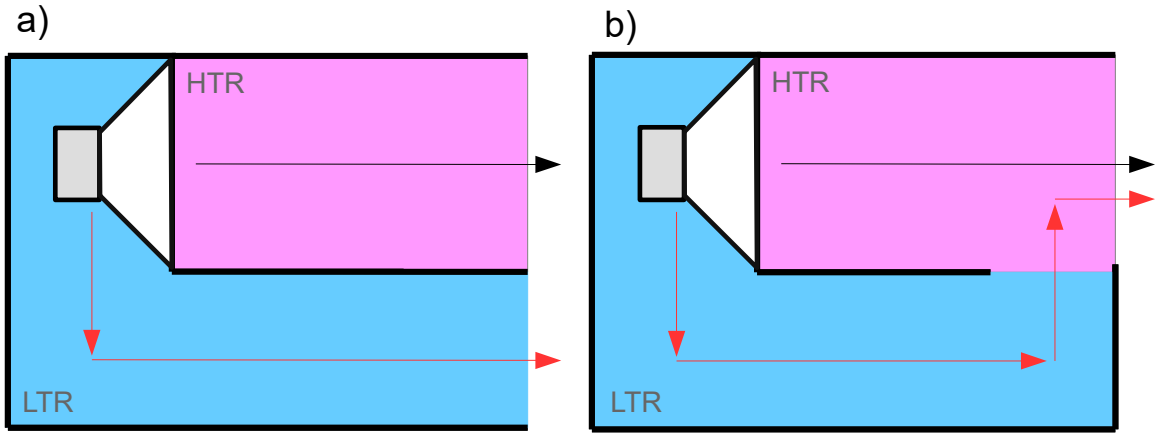

Figure 1.1: a) Parallel Transmission Line System, b) Paraflex Loudspeaker System

It consists of two quarter wave resonators, sitting at the front and back of the loudspeaker driver. Therefore, acoustic input of the resonators is out of phase by 180 deg. This configuration leads to the system operating similar to a parallel transmission line system, which is two separate transmission lines sitting at the front and back of the driver respectively as shown in figure 1.1 a). However, for "Paraflex" loudspeakers, both resonators crucially share the same mouth opening with a merge close to the output of the system, which is a major difference to every system having two parallel separate waveguides. This way, the total effective length of the so called "Low Tuned Resonator" (LTR) can be increased by the length shared with the so called "High Tuned Resonator" (HTR), which leads to lower tuning.
Different length of the HTR and LTR lead to different resonant frequencies, ideally increasing the overall bandwidth of the system if tuned strategically [1].
A lot of research has been done concerning "Transmission Line" loudspeaker systems, such as “An electroacoustic analysis of transmission line loudspeakers" by R. A. Robinson [2], providing theory on acoustic transmission lines in general as well as a very detailed model for acoustic

wave propagation in transmission lines filled with fibrous material. Also, works like “A computational model of transmission line loudspeakers" by J. Backman [3], dealing with solutions on how to compute system characteristics such as sound pressure output for parallel transmission line configurations as shown in figure 1.1 a). However, no research has been done taking into account merging transmission lines, sharing the same acoustic output as is the case for "Paraflex"-like configurations. Therefore, this work focuses on deriving a computational model for this kind of loudspeaker system, providing necessary information for simulation and development of "Paraflex" loudspeakers.

2 Loudspeaker Model

This chapter focuses on deriving a comprehensive model for loudspeaker enclosures, containing acoustic as well as mechanic and electric characteristics of the overall system. The modelling approach is based on analysis of the analogous electric circuit describing the system. Therefore, to make this work for "Paraflex" loudspeaker enclosures, it is necessary to find a method to transform the distributed acoustic elements of the quarter wave resonators into lumped elements in order to be able to perform electric circuit analysis on the model. This will be done by describing the quarter wave resonators as acoustic transmission lines, replacing the distributed line elements by their respective input impedance, which will be discussed in chapter 3.

2.1 Deriving the Electric Analogous Circuit

Figure 2.1 shows the electromechanoacoustic analogous circuit of a loudspeaker system, consisting of an electric, mechanic and acoustic domain with lumped elements.

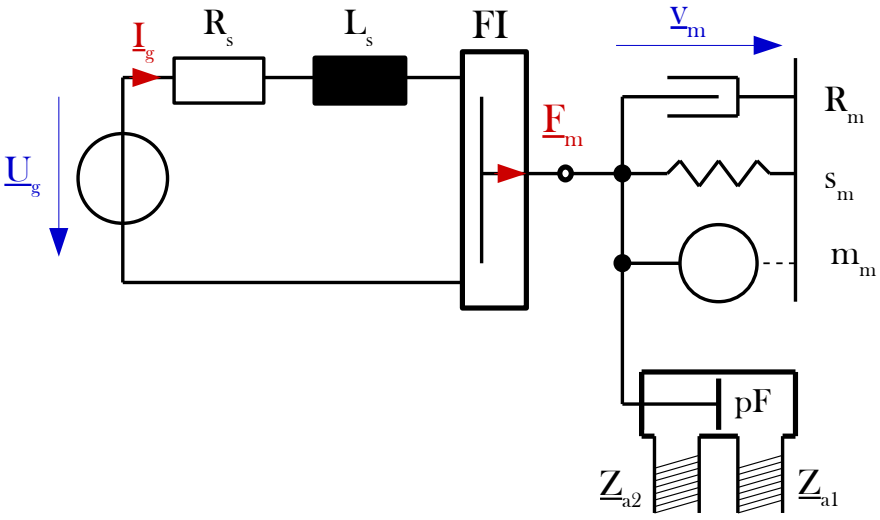

Figure 2.1: Electromechanoacoustic Analogous Circuit of a Loudspeaker System

The acoustic domain is modelled by some arbitrary impedances $\underline{Z}_{a1}$ and $\underline{Z}_{a2}$, sitting at the front and back of the pF converter. These impedances will later be replaced by the respective input impedances of the quarter wave resonators.
The mechanic domain of the loudspeaker driver is modelled by the elements R_m, s_m and m_m, which correspond to mechanic resistance, stiffness and mass respectively.
Also, the electric domain contains the voltage source $\underline{U}_g$ as well as the ohmic resistance of the loudspeaker voice coil R_s in series with its inductance L_s.

For this analogous circuit, pF and FI converters are used to link the respective acoustic, mechanic and electric domains. Elements from each domain can be transferred to the next domain by using the transformation constants of the converters as will be discussed in chapter 2.1.1 and 2.1.2.

2.1.1 Mechanoacoustic Conversion

Figure 2.2 shows the electromechanic analogous circuit of the loudspeaker system after mechanoacoustic conversion.

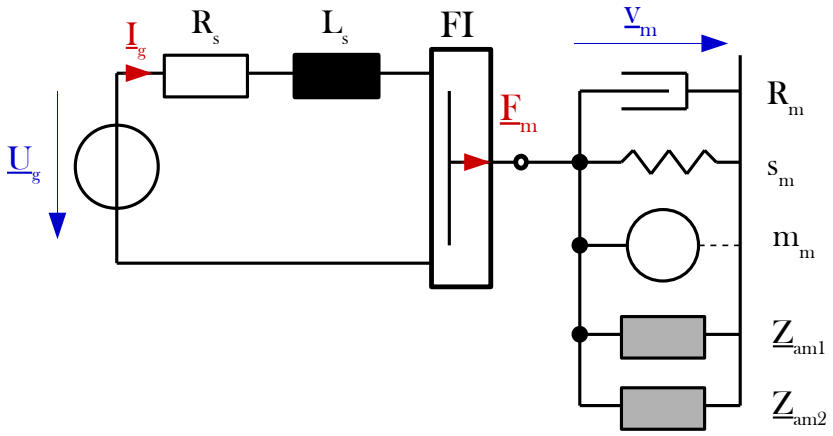

Figure 2.2: Electromechanic Analogous Circuit

With S_d being the area of the vibrating loudspeaker diaphragm, it is possible to transform the acoustic elements of figure 2.1 to the mechanic domain.
For an arbitrary acoustic impedance given by

$$\underline{Z}_a = \frac{\underline{p}}{\underline{q}} \tag{2.1}$$

the corresponding mechanic impedance is given by

$$\underline{Z}_a = \frac{\underline{p}}{\underline{q}} = \frac{\underline{F}}{\underline{v} \cdot S_d^2} = \frac{\underline{F}}{\underline{v}} \cdot \frac{1}{S_d^2} = \underline{Z}_m \cdot \frac{1}{S_d^2} \longrightarrow \underline{Z}_m = \underline{Z}_a \cdot S_d^2 \tag{2.2}$$

with

$\underline{p} = \frac{\underline{F}}{S_d}$ ... sound pressure
$\underline{q} = \underline{v} \cdot S_d$ ... volume velocity
$\underline{F}$ ... force
$\underline{v}$ ... velocity
$\underline{Z}_m$ ... mechanic impedance

Therefore, the transformed mechanic impedances $\underline{Z}_{am}$, corresponding to the impedances $\underline{Z}_a$ of the acoustic domain, can be calculated as follows:

$$\boxed{\underline{Z}_{am} = \underline{Z}_a \cdot S_d^2} \tag{2.3}$$

2.1.2 Electromechanic Conversion

With the electromechanic analogous circuit at hand, it is possible to use the FI converter to transfer all elements contained in the mechanic circuit of figure 2.2 to the electric domain. According to [4], mechanic components R_m, s_m and m_m can be transformed to equivalent electric resistance, inductance and capacitance R_{me}, L_{me} and C_{me} by making use of the FI converter as follows:

$$R_{me} = \frac{Bl^2}{R_m} \qquad L_{me} = \frac{Bl^2}{s_m} \qquad C_{me} = \frac{m_m}{Bl^2} \tag{2.4}$$

Bl ... force factor of the loudspeaker driver $\left[\frac{N}{A}\right]$

Also, with an arbitrary mechanic impedance being transformed as follows:

$$\underline{Z}_m = \frac{\underline{F}}{\underline{v}} = \frac{\underline{I} \cdot Bl^2}{\underline{U}} = \frac{\underline{I}}{\underline{U}} \cdot Bl^2 = \frac{1}{\underline{Z}_e} \cdot Bl^2 \longrightarrow \underline{Z}_e = \frac{Bl^2}{\underline{Z}_m} \tag{2.5}$$

with

$\underline{F} = \underline{I} \cdot Bl$

$\underline{v} = \dfrac{\underline{U}}{Bl}$

$\underline{I}$ ... electric current

$\underline{U}$ ... electric voltage

$\underline{Z}_e$ ... electric impedance

electric equivalents $\underline{Z}_{ae}$ of the acoustic impedances $\underline{Z}_a$ can be computed:

$$\boxed{\underline{Z}_{ae} = \frac{Bl^2}{\underline{Z}_{am}} = \frac{Bl^2}{\underline{Z}_a \cdot S_d^2}} \tag{2.6}$$

This leads to the final electric analogous circuit shown in figure 2.3.

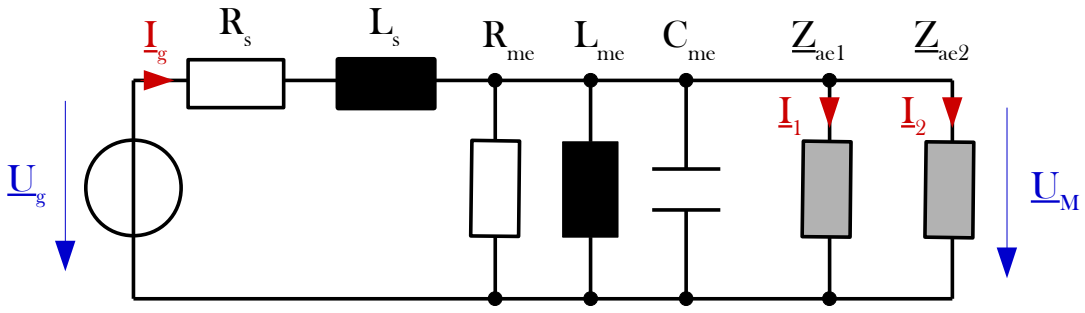

Figure 2.3: Electric Analogous Circuit

If impedances $\underline{Z}_{ae1}$ and $\underline{Z}_{ae2}$ are known, we can perform electric circuit analysis to obtain all wanted circuit quantities. This includes velocity of the loudspeaker diaphragm, which corresponds to voltage $\underline{U}_M$, or input sound pressure of the transmission lines corresponding to currents $\underline{I}_1$ and $\underline{I}_2$. In figure 2.3, the phase shift of 180° between front and back of the driver is not yet visible, but will be dealt with in chapter 4.
With the electric analogous circuit at hand, the next chapter discusses transmission line theory to obtain acoustic input impedance of a line.

3 Acoustic Transmission Line Theory

In this chapter, theory for acoustic transmission lines is discussed. This leads to sound pressure and acoustic impedance of the line dependent on location x in the line, which will then be utilized to calculate input impedance of the transmission lines as discussed in chapter 2 as well as acoustic output of the lines.

3.1 The Acoustic Transmission Line

Figure 3.1 shows an acoustic transmission line powered by a vibrating piston with velocity $\underline{v}_m$ at location $x = 0$.

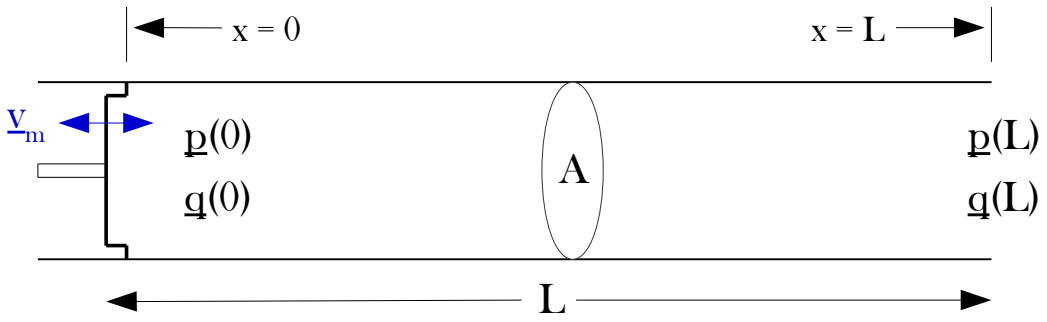

Figure 3.1: Acoustic Transmission Line

The line is of length L and terminates with acoustic impedance

$$\underline{Z}_a(L) = \frac{\underline{p}(L)}{\underline{q}(L)} \tag{3.1}$$

To derive the impedance and sound pressure distribution at any point x in the line, we discuss wave propagation in an acoustic transmission line by cutting it into very small segments and building the analogous electric circuit with respective acoustic elements.

3.2 Electroacoustic Solution

According to [2], an infinitesimal small line segment of length Δx can be described by the electric analogous circuit shown in figure 3.2.

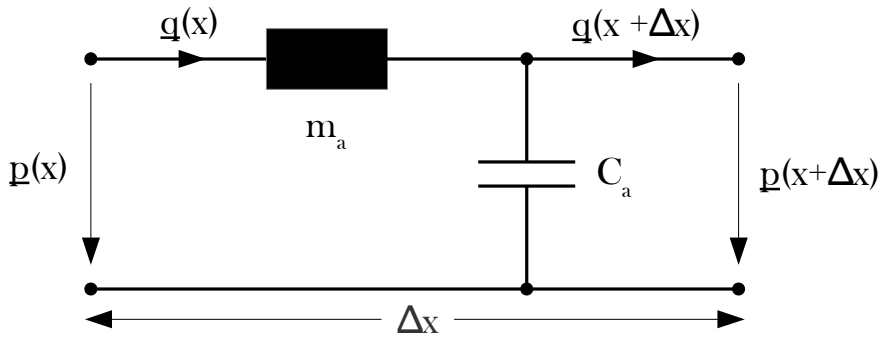

Figure 3.2: Infinitesimal Small Line Segment

In this circuit, m_a and C_a are the acoustical mass and compliance of the air enclosed in the respective line segment with length Δx, represented by the electric impedances of an inductor and capacitor respectively. According to [2], these can be calculated by multiplying the acoustic mass per unit length m_{ua} and compliance per unit length C_{ua} with the segment length Δx:

$$m_{ua} = \frac{\rho_0}{A} \Longrightarrow m_a = m_{ua} \cdot \Delta x \tag{3.2}$$

$$C_{ua} = \frac{A}{\rho_0 \cdot c^2} \Longrightarrow C_a = C_{ua} \cdot \Delta x \tag{3.3}$$

A ... cross sectional area of transmission line
ρ_0 ... air density
c ... sound propagation velocity

For harmonic oscillation, each line segment of length Δx can be described by the following equations:

$$\underline{p}(x + \Delta x) = \underline{p}(x) - \jmath\omega \cdot m_{ua}\Delta x \cdot \underline{q}(x) \tag{3.4}$$

$$\underline{q}(x + \Delta x) = \underline{q}(x) - \jmath\omega \cdot C_{ua}\Delta x \cdot \underline{p}(x + \Delta x) \tag{3.5}$$

By rearranging, we get:

$$\frac{\underline{p}(x + \Delta x) - \underline{p}(x)}{\Delta x} = -\jmath\omega m_{ua} \cdot \underline{q}(x) \tag{3.6}$$

$$\frac{\underline{q}(x + \Delta x) - \underline{q}(x)}{\Delta x} = -\jmath\omega C_{ua} \cdot \underline{p}(x + \Delta x) \tag{3.7}$$

By shrinking Δx to 0, we obtain the following differential equations:

$$\frac{d\underline{p}(x)}{dx} = -\jmath\omega m_{ua} \cdot \underline{q}(x) \tag{3.8}$$

$$\frac{d\underline{q}(x)}{dx} = -\jmath\omega C_{ua} \cdot \underline{p}(x) \tag{3.9}$$

Taking the second derivative, we get:

$$\frac{d^2\underline{p}(x)}{dx^2} = -\jmath\omega m_{ua} \cdot \frac{d\underline{q}(x)}{dx} \tag{3.10}$$

$$\frac{d^2\underline{q}(x)}{dx^2} = -\jmath\omega C_{ua} \cdot \frac{d\underline{p}(x)}{dx} \tag{3.11}$$

By substituting equations 3.8 and 3.9, we get:

$$\frac{d^2\underline{p}(x)}{dx^2} = -\omega^2 \cdot m_{ua} \cdot C_{ua} \cdot \underline{p}(x) \tag{3.12}$$

$$\frac{d^2\underline{q}(x)}{dx^2} = -\omega^2 \cdot C_{ua} \cdot m_{ua} \cdot \underline{q}(x) \tag{3.13}$$

This can be solved for $\underline{q}(x)$ and $\underline{p}(x)$ by making an educated guess as follows:

$$\underline{p}(x) = \underline{p}_{0+} \cdot \mathrm{e}^{-\underline{\Gamma}\cdot x} + \underline{p}_{0-} \cdot \mathrm{e}^{\underline{\Gamma}\cdot x} \tag{3.14}$$

$$\underline{q}(x) = \underline{q}_{0+} \cdot \mathrm{e}^{-\underline{\Gamma}\cdot x} + \underline{q}_{0-} \cdot \mathrm{e}^{\underline{\Gamma}\cdot x} \tag{3.15}$$

where

$\underline{p}_{0+}$ ... sound pressure amplitude of wave propagating in forward direction
$\underline{p}_{0-}$ ... sound pressure amplitude of wave propagating in backward direction
$\underline{q}_{0+}$ ... volume velocity amplitude of wave propagating in forward direction
$\underline{q}_{0-}$ ... volume velocity amplitude of wave propagating in backward direction
$\underline{\Gamma}$ ... propagation coefficient of the material in the line

Using 3.14 in equation 3.12, we get:

$$\underline{\Gamma}^2 \cdot \underline{p}(x) = -\omega^2 \cdot C_{ua} \cdot m_{ua} \cdot \underline{p}(x) \tag{3.16}$$

$$\underline{\Gamma}^2 = -\omega^2 \cdot C_{ua} \cdot m_{ua} \Longrightarrow \boxed{\underline{\Gamma} = \jmath\omega \cdot \sqrt{C_{ua} \cdot m_{ua}} = \jmath\omega \cdot \sqrt{\frac{A \cdot \rho_0}{A \cdot \rho_0 \cdot c^2}} = \jmath \cdot \frac{\omega}{c}} \tag{3.17}$$

Further, equation 3.14 needs to satisfy equation 3.8, so we get:

$$-\underline{\Gamma} \cdot \underline{p}_{0+} \cdot \mathrm{e}^{-\underline{\Gamma} \cdot x} + \underline{\Gamma} \cdot \underline{p}_{0-} \cdot \mathrm{e}^{\underline{\Gamma} \cdot x} = -\jmath\omega m_{ua} \cdot \underline{q}(x) \tag{3.18}$$

$$\begin{aligned} \underline{q}(x) = \frac{\underline{\Gamma}}{\jmath\omega m_{ua}} \cdot \underline{p}_{0+} \cdot \mathrm{e}^{-\underline{\Gamma} \cdot x} - \frac{\underline{\Gamma}}{\jmath\omega m_{ua}} \cdot \underline{p}_{0-} \cdot \mathrm{e}^{\underline{\Gamma} \cdot x} &= \frac{\underline{p}_{0+} \cdot A}{\rho_0 \cdot c} \cdot \mathrm{e}^{-\underline{\Gamma} \cdot x} - \frac{\underline{p}_{0-} \cdot A}{\rho_0 \cdot c} \cdot \mathrm{e}^{\underline{\Gamma} \cdot x} \\ &\stackrel{!}{=} \underline{q}_{0+} \cdot \mathrm{e}^{-\underline{\Gamma} \cdot x} + \underline{q}_{0-} \cdot \mathrm{e}^{\underline{\Gamma} \cdot x} \end{aligned} \tag{3.19}$$

This yields the following relations:

$$\boxed{\underline{q}_{0+} = \frac{\underline{p}_{0+} \cdot A}{\rho_0 \cdot c} = \frac{\underline{p}_{0+}}{Z_C}} \tag{3.20}$$

$$\boxed{\underline{q}_{0-} = -\frac{\underline{p}_{0-} \cdot A}{\rho_0 \cdot c} = -\frac{\underline{p}_{0-}}{Z_C}} \tag{3.21}$$

$$\boxed{Z_C = \frac{\rho_0 \cdot c}{A}} \tag{3.22}$$

where

Z_C...Characteristic impedance of acoustic line with cross sectional area A

3.2.1 Reflection Coefficient

If we want to find a solution for the acoustic impedance of the line $\underline{Z}_a(x)$ as well as acoustic pressure $\underline{p}(x)$, we first need to find $\underline{p}_{0-}$.
If we have a look at the boundary condition of the line where $x = L$, the following relation must hold:

$$\underline{Z}_a(L) = \frac{\underline{p}(L)}{\underline{q}(L)} = \frac{\underline{p}_{0+} \cdot \mathrm{e}^{-\underline{\Gamma} \cdot L} + \underline{p}_{0-} \cdot \mathrm{e}^{\underline{\Gamma} \cdot L}}{\underline{q}_{0+} \cdot \mathrm{e}^{-\underline{\Gamma} \cdot L} + \underline{q}_{0-} \cdot \mathrm{e}^{\underline{\Gamma} \cdot L}} = Z_C \cdot \frac{\underline{p}_{0+} \cdot \mathrm{e}^{-\underline{\Gamma} \cdot L} + \underline{p}_{0-} \cdot \mathrm{e}^{\underline{\Gamma} \cdot L}}{\underline{p}_{0+} \cdot \mathrm{e}^{-\underline{\Gamma} \cdot L} - \underline{p}_{0-} \cdot \mathrm{e}^{\underline{\Gamma} \cdot L}} \tag{3.23}$$

Solving for $\underline{p}_{0-}$, we get:

$$\boxed{\underline{p}_{0-} = \underline{p}_{0+} \cdot \frac{\underline{Z}_a(L) - Z_C}{\underline{Z}_a(L) + Z_C} \cdot \mathrm{e}^{-2\cdot\underline{\Gamma}\cdot L} = \underline{p}_{0+} \cdot \underline{r}_L \cdot \mathrm{e}^{-2\cdot\underline{\Gamma}\cdot L}} \tag{3.24}$$

$$\boxed{\underline{r}_L = \frac{\underline{Z}_a(L) - Z_C}{\underline{Z}_a(L) + Z_C}} \quad \ldots \text{ reflection coefficient at } x = L \tag{3.25}$$

3.2.2 Acoustic Impedance

With all this at hand, the acoustic impedance $\underline{Z}_a(x)$ at any arbitrary point x in the transmission line can be computed as follows:

$$\underline{Z}_a(x) = \frac{\underline{p}(x)}{\underline{q}(x)} = \frac{\underline{p}_{0+} \cdot \mathrm{e}^{-\underline{\Gamma}\cdot x} + \underline{p}_{0-} \cdot \mathrm{e}^{\underline{\Gamma}\cdot x}}{\underline{q}_{0+} \cdot \mathrm{e}^{-\underline{\Gamma}\cdot x} + \underline{q}_{0-} \cdot \mathrm{e}^{\underline{\Gamma}\cdot x}} = Z_C \cdot \frac{\underline{p}_{0+} \cdot \mathrm{e}^{-\underline{\Gamma}\cdot x} + \underline{p}_{0-} \cdot \mathrm{e}^{\underline{\Gamma}\cdot x}}{\underline{p}_{0+} \cdot \mathrm{e}^{-\underline{\Gamma}\cdot x} - \underline{p}_{0-} \cdot \mathrm{e}^{\underline{\Gamma}\cdot x}}$$

$$= Z_C \cdot \frac{\underline{p}_{0+} \cdot \mathrm{e}^{-\underline{\Gamma}\cdot x} + \underline{p}_{0+} \cdot \underline{r}_L \cdot \mathrm{e}^{-2\cdot\underline{\Gamma}\cdot L} \cdot \mathrm{e}^{\underline{\Gamma}\cdot x}}{\underline{p}_{0+} \cdot \mathrm{e}^{-\underline{\Gamma}\cdot x} - \underline{p}_{0+} \cdot \underline{r}_L \cdot \mathrm{e}^{-2\cdot\underline{\Gamma}\cdot L} \cdot \mathrm{e}^{\underline{\Gamma}\cdot x}} = Z_C \cdot \frac{\underline{p}_{0+} \cdot \mathrm{e}^{-\underline{\Gamma}\cdot x} \cdot \left(1 + \underline{r}_L \cdot \mathrm{e}^{-2\cdot\underline{\Gamma}\cdot L} \cdot \mathrm{e}^{2\cdot\underline{\Gamma}\cdot x}\right)}{\underline{p}_{0+} \cdot \mathrm{e}^{-\underline{\Gamma}\cdot x} \cdot (1 - \underline{r}_L \cdot \mathrm{e}^{-2\cdot\underline{\Gamma}\cdot L} \cdot \mathrm{e}^{2\cdot\underline{\Gamma}\cdot x})}$$

$$\boxed{\underline{Z}_a(x) = Z_C \cdot \frac{1 + \underline{r}_L \cdot \mathrm{e}^{-2\cdot\underline{\Gamma}\cdot(L-x)}}{1 - \underline{r}_L \cdot \mathrm{e}^{-2\cdot\underline{\Gamma}\cdot(L-x)}}} \tag{3.26}$$

This makes it possible to compute the acoustic input impedance $\underline{Z}_a(0)$ of the transmission line seen by the loudspeaker diaphragm only by knowing Z_C, the acoustic impedance $\underline{Z}_a(L)$ terminating the line as well as the length L of the line.

3.2.3 Acoustic Pressure

By making use of equation 3.14 and 3.24, we can solve for the acoustic pressure at any point x in the line:

$$\underline{p}(x) = \underline{p}_{0+} \cdot \left(\mathrm{e}^{-\underline{\Gamma}\cdot x} + \underline{r}_L \cdot \mathrm{e}^{-2\cdot\underline{\Gamma}\cdot L} \cdot \mathrm{e}^{\underline{\Gamma}\cdot x}\right) = \underline{p}_{0+} \cdot \mathrm{e}^{-\underline{\Gamma}\cdot x} \cdot \left(1 + \underline{r}_L \cdot \mathrm{e}^{-2\cdot\underline{\Gamma}\cdot(L-x)}\right) \tag{3.27}$$

To find $\underline{p}_{0+}$, we make use of the following relations:

$$\underline{Z}_a(0) \cdot \underline{q}(0) = \underline{p}(0) = \underline{p}_{0+} \cdot \left(1 + \underline{r}_L \cdot \mathrm{e}^{-2\cdot\underline{\Gamma}\cdot L}\right)$$

$$\longrightarrow \underline{p}_{0+} = \frac{\underline{Z}_a(0) \cdot \underline{q}(0)}{(1 + \underline{r}_L \cdot \mathrm{e}^{-2\cdot\underline{\Gamma}\cdot L})} \tag{3.28}$$

$$\boxed{\underline{p}(x) = \frac{\underline{Z}_a(0) \cdot \underline{q}(0)}{(1 + \underline{r}_L \cdot \mathrm{e}^{-2\cdot\underline{\Gamma}\cdot L})} \cdot \mathrm{e}^{-\underline{\Gamma}\cdot x} \cdot \left(1 + \underline{r}_L \cdot \mathrm{e}^{-2\cdot\underline{\Gamma}\cdot(L-x)}\right)} \tag{3.29}$$

If we now manage to obtain acoustic input impedance $\underline{Z}_a(0)$ with equation 3.26 as well as input volume velocity $\underline{q}(0)$ of the lines corresponding to $\underline{U}_M$ in figure 2.3, we are able to compute sound pressure $\underline{p}(x)$ at any point x in the line.

3.3 Transmission Line with Changing Cross Sectional Area

Figure 3.3 shows an acoustic transmission line with stepwise changing cross sectional area A as a function of x.

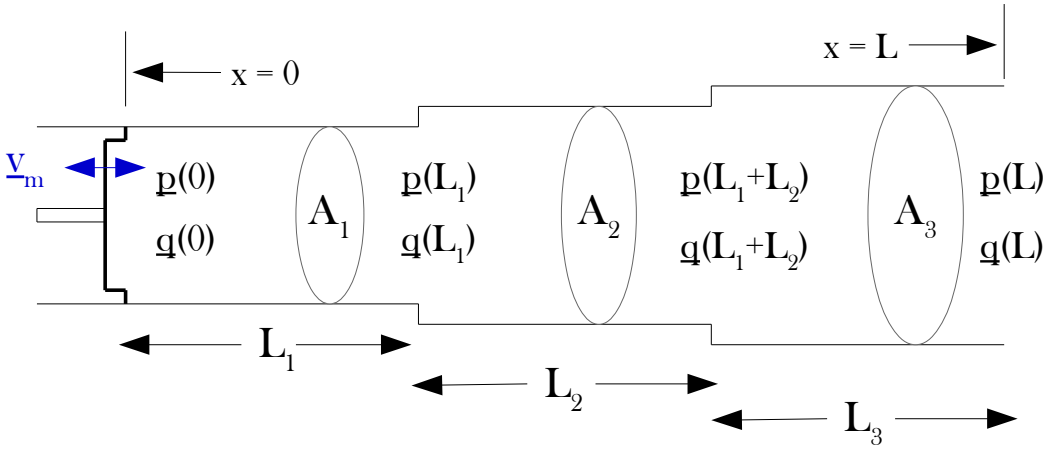

Figure 3.3: Stepped Transmission Line

This can be modelled as a cascade of line segments, each with different area and therefore different characteristic acoustic impedance Z_C.
By applying computations derived in chapter 3.2, [3] suggests that this cascade can be analysed by starting with the segment closest to the open end of the line, computing its input impedance and then using it as the load to the next line segment. This way, input impedance of the whole line can be computed. Acoustic sound pressure and volume velocity can be obtained by starting at the line segment closest to the input of the overall line, computing its output pressure and volume velocity, using it as input to the next line segment, continuing respectively.

4 Paraflex Loudspeaker Analysis

By applying the knowledge gained from chapter 3, the following chapter first focuses on obtaining the acoustic input impedance of the HTR and LTR of a "Paraflex" loudspeaker. This then is used to perform electric circuit analysis of the electric analogous circuit derived in chapter 2, which leads to the overall electric impedance of the system seen by the voltage source, as well as diaphragm velocity and input sound pressure to the lines.
Eventually, acoustic output pressure of the lines can be computed, leading to sound pressure response of the overall system. Therefore, after discussing the necessary computational steps, we are able to obtain all the wanted system characteristics from the model.

4.1 Paraflex System Setup

Figure 4.1 shows a general "Paraflex" system, consisting of two quarter wave resonators that are linked at an arbitrary point x_J. The transmission lines with length L_1 and L_3 correspond to the HTR and the line with length L_2 to the LTR respectively. Also, L_3 corresponds to the shared length mentioned in chapter 1, increasing the total length of the LTR.

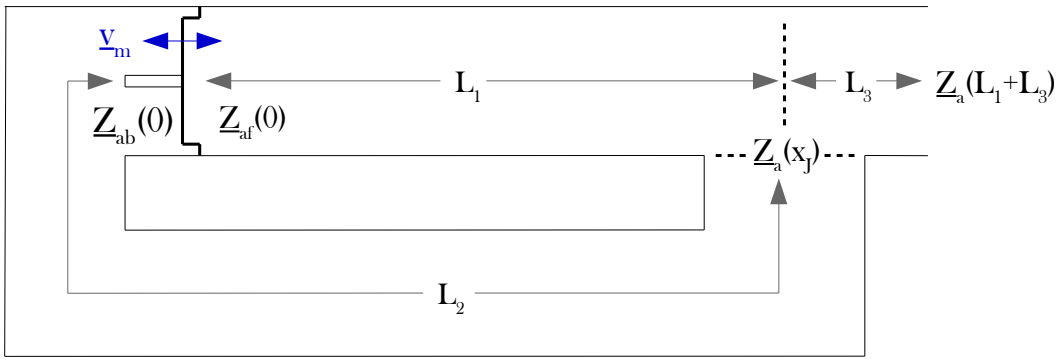

Figure 4.1: Paraflex System

This system can be decomposed into three transmission lines as shown in figure 4.2.

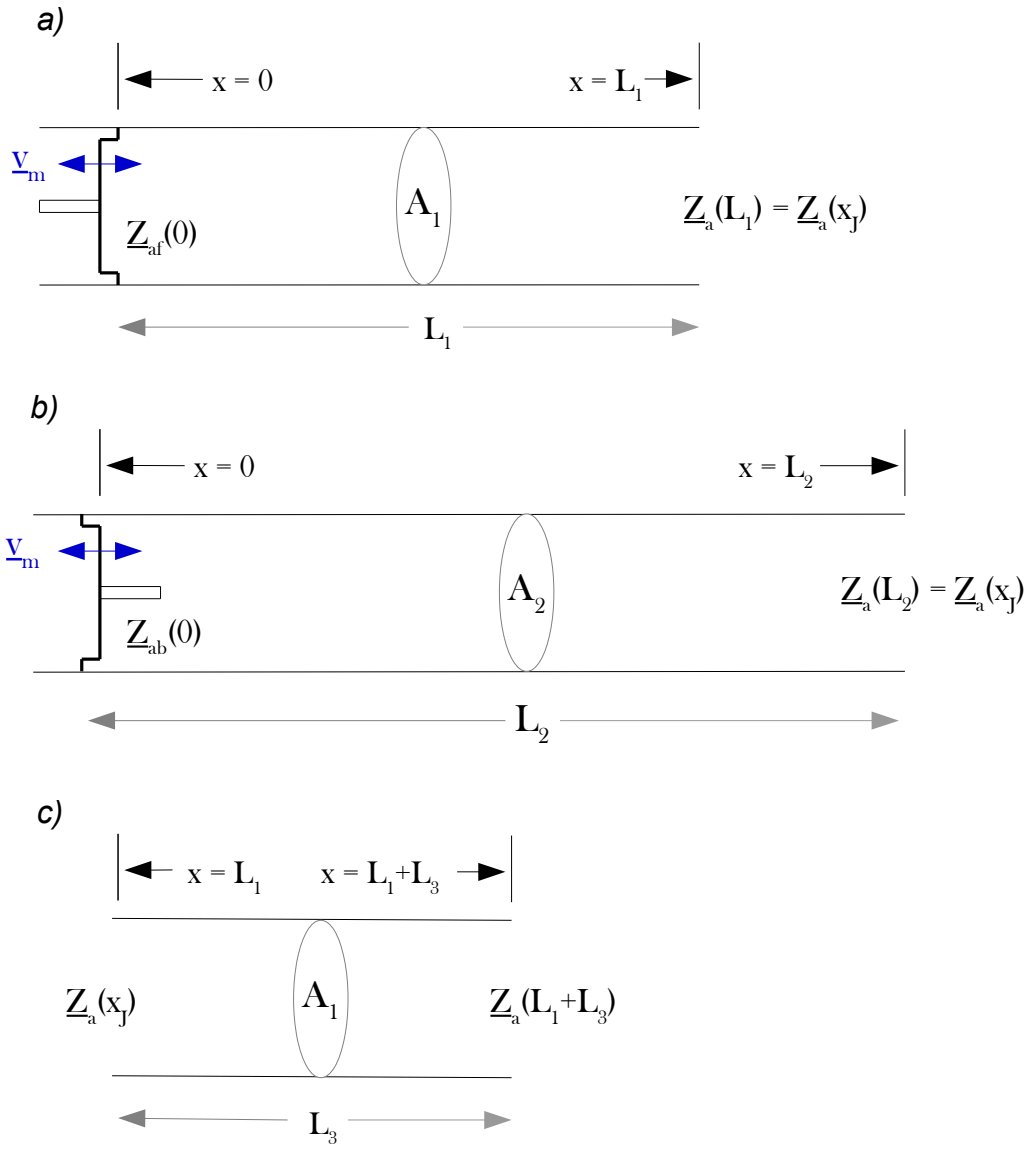

Figure 4.2: a) High Tuned Resonator Transmission Line b) Low Tuned Resonator Transmission Line c) Shared Transmission Line

The HTR is composed of two distinct acoustic transmission lines. The first one is of length L_1 with cross sectional area $A_1 \geq S_d$ and acoustic impedance $\underline{Z}_a(x_J)$ at point $x = L_1$ where the LTR merges into the HTR.
The second one is of length L_3 with same cross sectional area A_1 and acoustic input impedance $\underline{Z}_a(x_J)$ as well as load impedance $\underline{Z}_a(L_1 + L_3)$.

The LTR is of length L_2 ($L_2 > L_1 > L_3$) with cross sectional area $A_2 \geq S_d$ and acoustic impedance $\underline{Z}_a(x_J)$ at point $x = L_2$ which is the same point as $x = L_1$ in the HTR. Therefore, $\underline{Z}_a(x_J)$ is the acoustic impedance linking the three separate transmission lines.

In the following, these three resonator systems will be used to calculate acoustic input impedances to the lines $\underline{Z}_{af}(0)$ and $\underline{Z}_{ab}(0)$. This then will lead to acoustic volume velocity by analysis of the electric analogous circuit which eventually enables us to compute sound pressure at the output of the overall system by making use of equations derived in chapter 3 while matching the interface conditions of the two resonators.

4.2 HTR and LTR Impedances

Acoustic input impedance $\underline{Z}_{af}(0)$ of the HTR can be computed with equation 3.26. For this, it is necessary to know the acoustic impedance $\underline{Z}_a(L_1+L_3)$ terminating the line. As the open end of the system is assumed to sit in an infinite baffle, its acoustic impedance given by [4] can be used:

$$\underline{Z}_a(L_1+L_3) = \frac{\underline{p}(L_1+L_3)}{\underline{q}(L_1+L_3)} = \underline{Z}_{ib} = \frac{Z_0}{A_1} \cdot \left[1 - 2 \cdot \frac{J_1(2ka)}{2ka} + 2\jmath \cdot \frac{H_1(2ka)}{2ka}\right] \tag{4.1}$$

where

$\underline{p}(L_1+L_3)$ ... complex sound pressure at $x = L_1+L_3$
$\underline{q}(L_1+L_3)$ ... complex volume velocity at $x = L_1+L_3$
$Z_0 = \rho_0 \cdot c$ ... acoustic impedance of a plane wave
J_1 ... Bessel function of first order
H_1 ... Struve function of first order
k ... wave number
a ... radiating area radius

With this, we are able to calculate $\underline{Z}_{af}(0)$ as follows:

$$\underline{r}_{L_3} = \frac{\underline{Z}_{ib} - Z_{C_1}}{\underline{Z}_{ib} + Z_{C_1}} \quad \text{with} \quad Z_{C_1} = \frac{Z_0}{A_1} \tag{4.2}$$

$$\boxed{\underline{Z}_{af}(0) = Z_{C_1} \cdot \frac{1 + \underline{r}_{L_3} \cdot \mathrm{e}^{-2\cdot\underline{\Gamma}\cdot(L_1+L_3)}}{1 - \underline{r}_{L_3} \cdot \mathrm{e}^{-2\cdot\underline{\Gamma}\cdot(L_1+L_3)}}} \tag{4.3}$$

As the LTR with length L_2 joins the HTR at x_J, to compute $\underline{Z}_{ab}(0)$ we first need to calculate acoustic impedance $\underline{Z}_a(x_J)$, which is the termination impedance seen by the LTR. Using equation 3.26, we get

$$\underline{Z}_a(x_J) = Z_{C_1} \cdot \frac{1 + \underline{r}_{L_3} \cdot \mathrm{e}^{-2\cdot\underline{\Gamma}\cdot L_3}}{1 - \underline{r}_{L_3} \cdot \mathrm{e}^{-2\cdot\underline{\Gamma}\cdot L_3}} \tag{4.4}$$

Now, $\underline{Z}_{ab}(0)$ can be computed by again using equation 3.26, with $\underline{Z}_a(x_J)$ being the termination impedance of the LTR:

$$\underline{r}_{L_2} = \frac{\underline{Z}_a(x_J) - Z_{C_2}}{\underline{Z}_a(x_J) + Z_{C_2}} \quad \text{with} \quad Z_{C_2} = \frac{Z_0}{A_2} \tag{4.5}$$

$$\boxed{\underline{Z}_{ab}(0) = Z_{C_2} \cdot \frac{1 + \underline{r}_{L_2} \cdot \mathrm{e}^{-2\cdot\underline{\Gamma}\cdot L_2}}{1 - \underline{r}_{L_2} \cdot \mathrm{e}^{-2\cdot\underline{\Gamma}\cdot L_2}}} \tag{4.6}$$

4.3 Electric Analogous Circuit Analysis

Figure 4.3 again shows the electric analogous circuit obtained in chapter 2.
The arbitrary impedances $\underline{Z}_{ae1}$ and $\underline{Z}_{ae2}$ transformed in chapter 2 have now been replaced by the known electric impedances $\underline{Z}_{TL1e}$ and $\underline{Z}_{TL2e}$, which correspond to the input impedance of the HTR $\left[\underline{Z}_{af}(0)\right]$ and LTR $[\underline{Z}_{ab}(0)]$, calculated with equation 4.3 and 4.6 respectively. Therefore, we now are able to perform electric circuit analysis to obtain $\underline{U}_M$, $\underline{I}_{TL1}$ and $\underline{I}_{TL2}$ as well as total electric input impedance $\underline{Z}_e$.

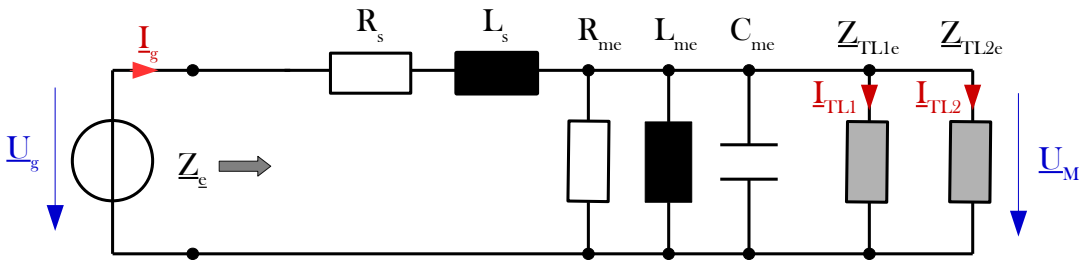

Figure 4.3: Electric Analogous Circuit

4.3.1 Electric Input Impedance

Total electric input impedance $\underline{Z}_e$ is given by the series combination of elements R_s and L_s with the parallel circuit of elements R_{me}, L_{me}, C_{me}, $\underline{Z}_{TL1e}$ and $\underline{Z}_{TL2e}$. The simplified circuit is shown in figure 4.4.

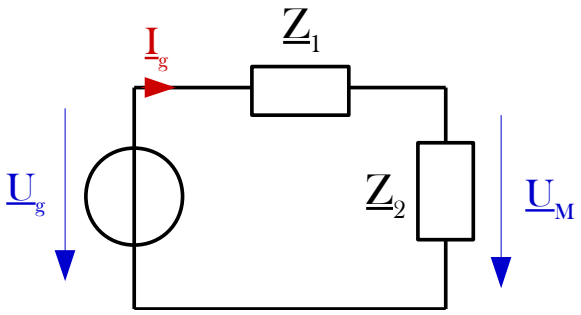

Figure 4.4: Simplified Electric Analogous Circuit

Admittance $\underline{Y}_2$ of the parallel circuit is given by:

$$\underline{Y}_2 = \frac{1}{R_{me}} + \frac{1}{\jmath\omega L_{me}} + \jmath\omega C_{me} + \frac{1}{\underline{Z}_{TL1e}} + \frac{1}{\underline{Z}_{TL2e}} \tag{4.7}$$

As

$$\underline{Z}_1 = R_s + \jmath\omega L_s \tag{4.8}$$

the total electric input impedance of the circuit is given by:

$$\boxed{\underline{Z}_e = \underline{Z}_1 + \underline{Z}_2 = \underline{Z}_1 + \frac{1}{\underline{Y}_2} = R_s + \jmath\omega L_s + \frac{1}{\frac{1}{R_{me}} + \frac{1}{\jmath\omega L_{me}} + \jmath\omega C_{me} + \frac{1}{\underline{Z}_{TL1e}} + \frac{1}{\underline{Z}_{TL2e}}}} \tag{4.9}$$

4.3.2 Acoustic Input Volume Velocity and Sound Pressure

In figure 4.4, $\underline{U}_M$ corresponds to the diaphragm velocity of the loudspeaker driver or the input volume velocity $\underline{q}(0)$ to the lines. It can be computed by applying a voltage divider as follows:

$$\underline{U}_M = \underline{U}_g \cdot \frac{\underline{Z}_2}{\underline{Z}_1 + \underline{Z}_2} \tag{4.10}$$

With

$$\underline{v}_M = \frac{\underline{U}_M}{Bl} \tag{4.11}$$

and

$$\underline{q}(0) = \underline{v}_M \cdot S_d \tag{4.12}$$

we get

$$\boxed{\underline{q}(0) = \underline{U}_g \cdot \frac{\underline{Z}_2}{\underline{Z}_1 + \underline{Z}_2} \cdot \frac{S_d}{Bl}} \tag{4.13}$$

As $\underline{U}_M$ is the voltage drop over $\underline{Z}_{TL1e}$ and $\underline{Z}_{TL2e}$, we can make use of Ohm's Law to compute $\underline{I}_{TL1}$ and $\underline{I}_{TL2}$:

$$\underline{I}_{TLi} = \frac{\underline{U}_M}{\underline{Z}_{TLie}} \tag{4.14}$$

Therefore, since

$$\underline{F}_{TLi} = \underline{I}_{TLi} \cdot Bl \tag{4.15}$$

and

$$\underline{p}_{TLi} = \frac{\underline{F}_{TLi}}{S_d} \tag{4.16}$$

we are able to compute input sound pressure to the HTR ($\underline{p}_{TL1}$) and input sound pressure to the LTR ($\underline{p}_{TL2}$) as follows:

$$\boxed{\underline{p}_{TLi} = \frac{\underline{U}_M}{\underline{Z}_{TLie}} \cdot \frac{Bl}{S_d}} \tag{4.17}$$

This enables us to compute sound pressure at the output of the lines as will be discussed in the next chapter, using equation 4.13 for $\underline{q}(0)$ in equation 4.18 and 4.19. As input volume velocity to the lines is inverted by 180°, this has to be taken into account by applying a negative sign to $\underline{q}(0)$ for one of the resonators, as done in equation 4.19.

4.4 Output Sound Pressure

As discussed in chapter 3.2, output sound pressure of a transmission line with given input can be calculated using equation 3.29.
As for a "Paraflex" system, the LTR joins with the HTR at point x_J, we have to compute sound pressure of both lines at this point of interest:

$$\underline{p}_{L_1}(x_J) = \underline{p}_{L_1}(L_1) = \frac{\underline{Z}_{af}(0) \cdot \underline{q}(0)}{\left(1 + \underline{r}_{L_1} \cdot \mathrm{e}^{-2 \cdot \underline{\Gamma} \cdot L_1}\right)} \cdot \mathrm{e}^{-\underline{\Gamma} \cdot L_1} \cdot \left(1 + \underline{r}_{L_1}\right), \quad \underline{r}_{L_1} = \frac{\underline{Z}_a(x_J) - Z_{C_1}}{\underline{Z}_a(x_J) + Z_{C_1}} \tag{4.18}$$

$$\underline{p}_{L_2}(x_J) = \underline{p}_{L_2}(L_2) = \frac{\underline{Z}_{ab}(0) \cdot (-\underline{q}(0))}{\left(1 + \underline{r}_{L_2} \cdot \mathrm{e}^{-2 \cdot \underline{\Gamma} \cdot L_2}\right)} \cdot \mathrm{e}^{-\underline{\Gamma} \cdot L_2} \cdot \left(1 + \underline{r}_{L_2}\right), \quad \underline{r}_{L_2} = \frac{\underline{Z}_a(x_J) - Z_{C_2}}{\underline{Z}_a(x_J) + Z_{C_2}} \tag{4.19}$$

The total pressure at $x = x_J$ is then given by the complex sum of both lines:

$$\underline{p}(x_J) = \underline{p}_{L_1}(L_1) + \underline{p}_{L_2}(L_2) \tag{4.20}$$

Finally, it is possible to compute total acoustic output of the system by again making use of equation 3.29, with L_3 being the length of the remaining line from point $x = L_1$ to point $x = L_1 + L_3$ and $\underline{Z}_a(x_J)$ being its input impedance as well as $\underline{q}(x_J)$ being its input volume velocity at $x = x_J$:

$$\underline{q}(x_J) = \frac{\underline{p}(x_J)}{\underline{Z}_a(x_J)} \tag{4.21}$$

$$\boxed{\underline{p}(L_3) = \frac{\underline{Z}_a(x_J) \cdot \underline{q}(x_J)}{\left(1 + \underline{r}_{L_3} \cdot \mathrm{e}^{-2 \cdot \underline{\Gamma} \cdot L_3}\right)} \cdot \mathrm{e}^{-\underline{\Gamma} \cdot L_3} \cdot \left(1 + \underline{r}_{L_3}\right)} \tag{4.22}$$

4.5 Output Sound Pressure at One Meter

For representative comparison of the sound pressure level generated by different loudspeaker cabinets, output sound pressure is usually computed at one meter distance from the system output. According to [2], for a known volume velocity $\underline{q}(r = 0)$ at the system output sitting in an infinite baffle, the sound pressure at distance r is given by:

$$\underline{p}(r) = \jmath\omega\rho_0 \cdot \underline{q}(r = 0) \cdot \frac{\mathrm{e}^{-\jmath \cdot k \cdot r}}{2\pi r} \tag{4.23}$$

The volume velocity $\underline{q}(r = 0)$ at the output can be computed using the output sound pressure of the system $\underline{p}(L_1 + L_3)$ obtained with equation 4.22 and the acoustic load impedance $\underline{Z}_{ib}$:

$$\underline{q}(r = 0) = \frac{\underline{p}(L_1 + L_3)}{\underline{Z}_{ib}} \tag{4.24}$$

Therefore, we are able to compute sound pressure at one meter distance from the system output $\underline{p}(1)$ as follows:

$$\boxed{\underline{p}(1) = \jmath\omega\rho_0 \cdot \underline{q}(r=0) \cdot \frac{\mathrm{e}^{-\jmath\cdot k}}{2\pi} = \jmath\omega\rho_0 \cdot \frac{\underline{p}(L_1+L_3)}{\underline{Z}_{ib}} \cdot \frac{\mathrm{e}^{-\jmath\cdot k}}{2\pi}} \tag{4.25}$$

Eventually, sound pressure level can be computed:

$$\boxed{L_p = 20 \cdot \log\left(\frac{\left|\underline{p}(1)\right|}{p_0}\right)} \tag{4.26}$$

$p_0 = 20$ µPa ... reference sound pressure

5 Simulation Results

After obtaining the necessary equations to compute sound pressure as well as acoustic impedance of a transmission line system at any point of interest and applying computations to the more complex model of a "Paraflex" system, this chapter presents simulation results for two distinct test cases. First, a very simple configuration of an acoustic transmission line loudspeaker system is simulated to build deeper understanding for how quarter wave resonators work. Consequently, the second test case treats a "Paraflex" loudspeaker configuration as described in chapter 4.

5.1 Simulation of a Transmission Line System

Figure 5.1 shows the configuration of the transmission line system for the first test case. The front side of the membrane as well as the output end of the acoustic transmission line are assumed to sit in an infinite baffle, therefore acoustic impedance at those points of interest must be equal to the acoustic impedance described in equation 4.1. Changes for Z_{ib} due to interaction between both outputs are neglected. The line is of two meters length with the shape of a cylindrical tube and cross sectional area of $1000\,\mathrm{cm}^2$ (equal to a diameter of $d = 36$ cm). The bend in the transmission line is assumed not to have any effects on acoustic performance of the transmission line.

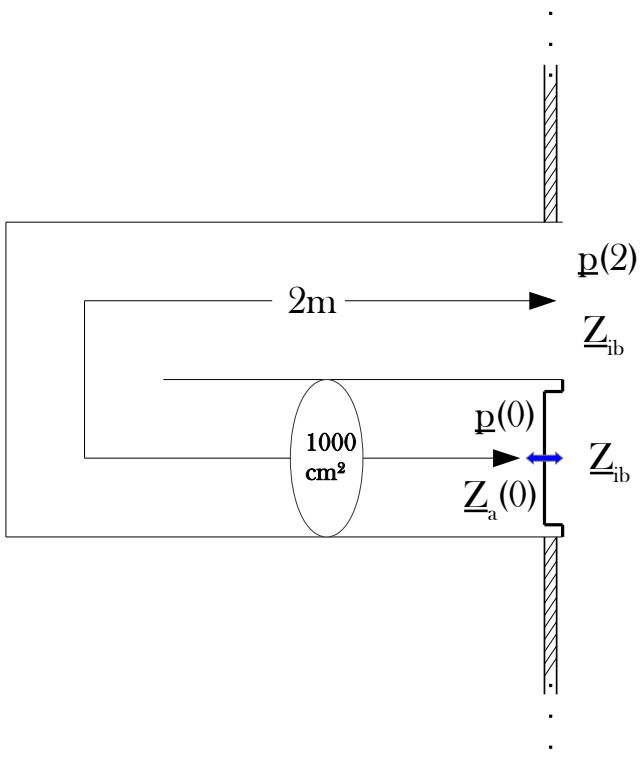

Figure 5.1: Simulated Transmission Line System

The transmission line system is powered by a loudspeaker driver with the following parameters:

$S_d = 841 \text{ cm}^2$ ($d = 33$ cm)
$Bl = 26.7 \frac{N}{A}$
$M_{md} = 162$ g
$C_{ms} = 90 \frac{\mu\text{m}}{N}$
$R_{ms} = 4.4 \frac{\text{kg}}{\text{s}}$
$R_s = 5.4\ \Omega$
$L_s = 1.6\ mH$

Input peak voltage of the voltage source $\underline{U}_g$ is equal to one volt.

5.1.1 Acoustic Input Impedance

Figure 5.2 shows the absolute value of the acoustic input impedance to the line $\underline{Z}_a(0)$ computed with equation 3.26.

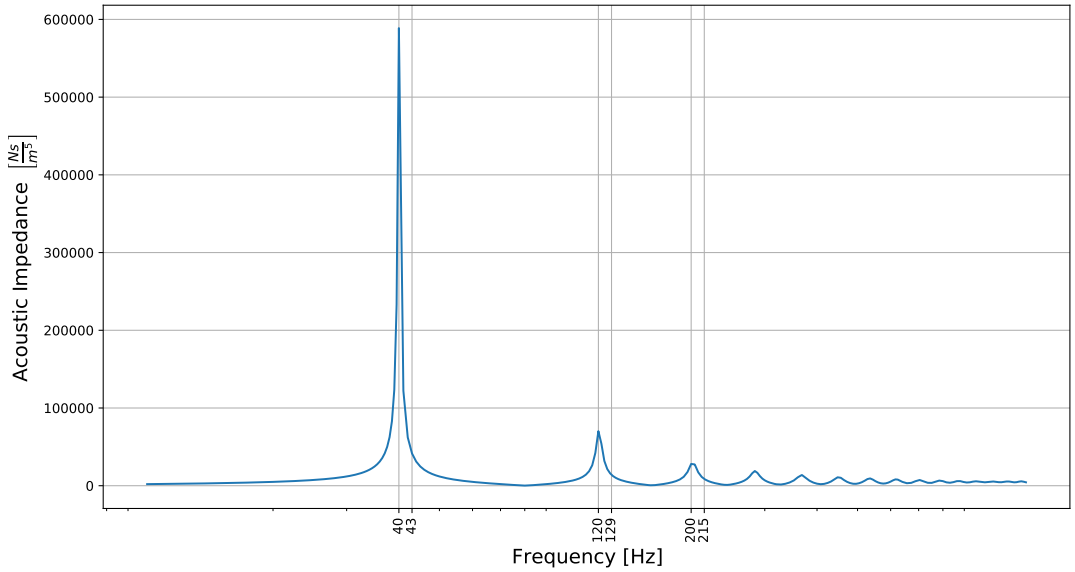

Figure 5.2: Acoustic Input Impedance of the Transmission Line System

Distinct peaks in amplitude can be observed, which correspond to the resonant frequencies of the line. As mentioned before, quarter wave resonators are designed to resonate at frequencies where the length of the line corresponds to odd multiples of their quarter wave lengths. These can be calculated as follows:

$$f_k = \frac{(2k+1) \cdot c}{4 \cdot L}, \qquad k \in \mathbb{N}_0 \tag{5.1}$$

This results in resonant frequencies that are odd multiples of 43 Hz for the line with length $L = 2$ in figure 5.1:

$$f_k = \frac{(2k+1) \cdot 344}{4 \cdot 2} = (2k+1) \cdot 43 \tag{5.2}$$

However, resonance peaks in figure 5.2 appear at frequencies slightly shifted down from the ones calculated in equation 5.2.
If we have a look at equation 3.24, the reflected wave $\underline{p}_{0-}$ experiences a phase shift at the open end of the line, dependent on the reflection coefficient $\underline{r}_L$. For low frequencies ($\ll 40$ Hz), as the real part of the load impedance $\underline{Z}_a(L) = \underline{Z}_{ib}$ is much smaller then the characteristic impedance Z_C of the line, the reflection coefficient $\underline{r}_L$ given by equation 3.25 approximately equals -1, which is equal to a phase shift of 180° for the reflected sound pressure wave. A phase shift of 180° leads to positive sound pressure interference and consequently series resonance at $x = 0$ for frequencies with quarter wavelength equal to the length of the line, as this leads to the reflected sound pressure wave arriving at $x = 0$ after the membrane has done half a cycle (corresponding to 180° phase shift), therefore adding up in phase with the membrane oscillation.
However, for the fundamental resonant frequency of the line at 40 Hz and frequencies above, the reflection coefficient adds less phase shift to the reflected wave, as the load impedance starts to increase. Subsequently, resonance happens at frequencies slightly lower than the expected quarter wave frequency, as for positive interference of sound pressure at $x = 0$, the loudspeaker membrane now needs to travel less than half a cycle for membrane oscillation and reflected sound pressure wave to add up in phase at $x = 0$. Table 5.1 shows the reflection coefficients and corresponding phase shift for the first three resonant frequencies of the transmission line system in figure 5.1.

f_r	$\underline{r}_L(f_r)$	$\angle\underline{r}_L(f_r)$
40	$-0.96 + \jmath \cdot 0.21$	167.3°
120	$-0.71 + \jmath \cdot 0.5$	144.3°
200	$-0.43 + \jmath \cdot 0.59$	125.5°

Table 5.1: Reflection Coefficient at Resonant Frequencies f_r

For these to be resonant frequencies, the membrane needs to experience the same phase change as the reflected wave in the time needed for the sound pressure wave to propagate forth and back through the line so both add up in phase. Therefore, these frequencies need to satisfy the following equation:

$$\angle\underline{r}_L(f_r) \stackrel{!}{=} \frac{2 \cdot L}{c} \cdot 360° \cdot f_r \tag{5.3}$$

where

$\angle\underline{r}_L(f_r)$ ... phase shift of the reflected wave at f_r

$\frac{2 \cdot L}{c}$ ... time needed for forward and backward propagation

$360° \cdot f_r$ ... membrane phase shift per second at f_r

The first three resonant frequencies have been highlighted in figure 5.2. A small deviation in phase shift for equation 5.3 due to numerical errors can be neglected. Note how the absolute shift in frequency compared to resonant frequencies calculated with equation 5.1 increases for higher resonant frequencies. This is due to the load impedance approaching the characteristic impedance of the line and therefore less phase shift being added to the reflected wave, resulting in lower resonant frequency as mentioned above.

5.1.2 Electric Input Impedance

Figure 5.3 shows the absolute value of the electric input impedance of the system computed with equation 4.9, where the electric equivalent of the acoustic impedance of a vibrating piston in an infinite baffle $\underline{Z}_{ib}$ has been used for $\underline{Z}_{TL2e}$ and the electric equivalent of the acoustic input impedance to the transmission line $\underline{Z}_a(0)$ calculated with equation 3.26 has been used for $\underline{Z}_{TL1e}$ in figure 4.3. These correspond to the acoustic impedance sitting at the back and front of the membrane respectively. The electric equivalents of the acoustic impedance faced by the membrane as well as mechanic impedance of the loudspeaker driver are shown as well.

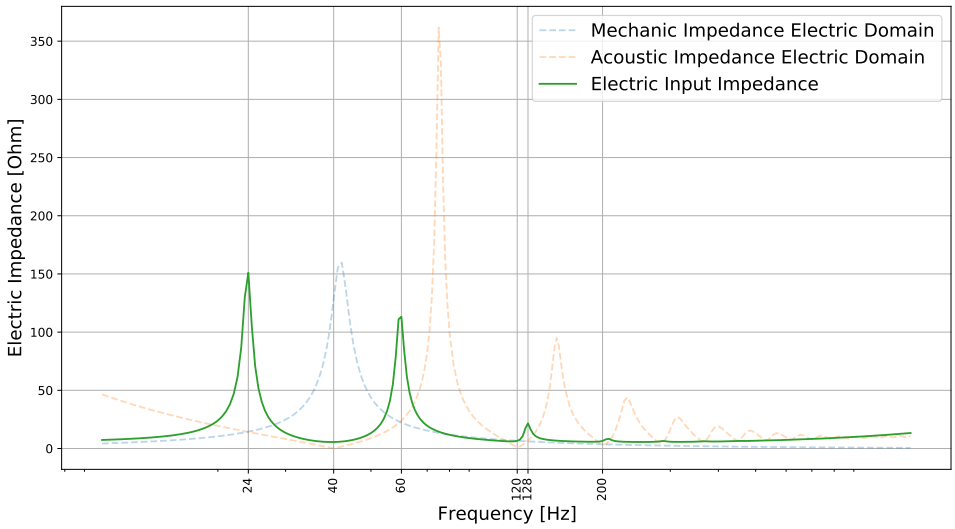

Figure 5.3: Total Electric Input Impedance of the Transmission Line System and Electric Equivalents of Acoustic and Mechanic Impedances

Again, distinct peaks in amplitude can be observed, with the first three peaks sitting at 24 Hz, 60 Hz and 128 Hz. As with a simple loudspeaker driver in free air, peaks in electric impedance are caused by backward induced electric current due to large driver motion. As can be seen in figure 4.3, total electric impedance $\underline{Z}_e$ corresponds to the series resistance of the drivers voice coil elements and the parallel circuit of mechanic and acoustic impedance equivalents in the electric domain. This results in low or high total electric impedance where the parallel combination of acoustic and mechanic impedance equivalents is low or high respectively. Subsequently, peaks of total electric impedance and therefore high driver motion at these frequencies dependent on the relation of mechanic impedance resonance of the driver and acoustic impedance resonancies of the transmission line. Also we can observe that at the resonant frequencies of the acoustic input impedance to the line of 40 Hz, 120 Hz and 200 Hz found in chapter 5.1.1, the electric input impedance is at a minimum which means there is minimum membrane motion at this point. Here, total impedance of the parallel circuit is dominated by the acoustic impedance equivalent in the electric domain which leads to low driver motion due to high acoustic input impedance to the line at this particular frequencies, opposing the drivers motion.

5.1.3 Input and Output Sound Pressure

Figure 5.4 shows the input and output sound pressure of the transmission line corresponding to $\underline{p}(0)$ and $\underline{p}(2)$ in figure 5.1, computed with equation 3.29.

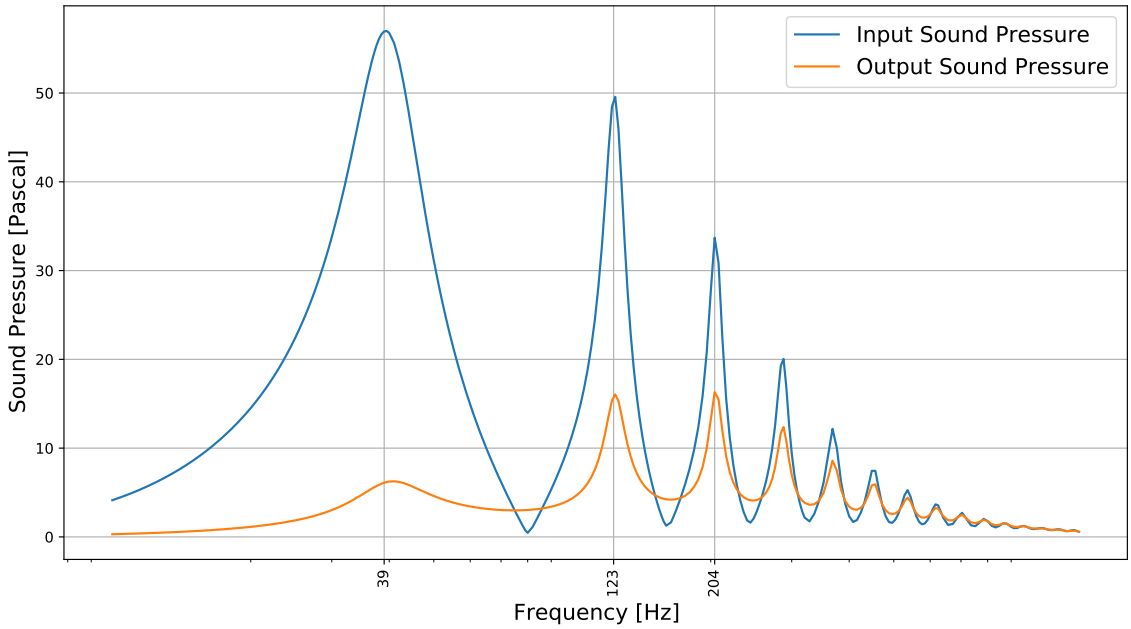

Figure 5.4: Input and Output Sound Pressure of the Transmission Line

For the input as well as output sound pressure of the line, we can observe resonance at 39 Hz, 123 Hz and 204 Hz, which are about the resonant frequencies found in chapter 5.1.1. The slight shift in frequency of about 1 Hz, 3 Hz and 4 Hz respectively will need further investigation, as this exceeds the limits of this work. As at low frequencies, most of the sound pressure wave is reflected at the open end of the line, there is a rather big difference in amplitude of input and output sound pressure. With increasing frequency though, there is less reflection and the output sound pressure approaches that at the input of the line.

5.1.4 Sound Pressure Level at One Meter

Figure 5.5 shows the sound pressure level of the front of the driver at one meter distance and the output of the transmission line at one meter distance, computed with equation 4.25 and 4.26. If we assume both the membrane and the open end of the line to have equal distance of one meter to the point of interest, we can compute the total sound pressure level at this point by using the complex sum of both sound pressures at this point for $\underline{p}(1)$ in equation 4.26. This is also shown in figure 5.5.

At the frequencies of high sound pressure at the output of the transmission line found in chapter 5.1.3, total system sound pressure is dominated by the transmission line. At the resonant frequencies found in chapter 5.1.1, the membrane is facing high acoustic impedance which leads to low membrane movement and therefore low sound pressure output at the front of the driver. However, resonance in the line still leads to high output of the overall system, clearly visible in the total sound pressure response with peaks repeating for every frequency of high sound pressure output found in figure 5.4. As can be seen in figure 5.5, the working bandwidth of a "Transmission Line" loudspeaker as shown in figure 5.1 is limited to about the second resonant frequency of the line, as there is a significant dip in sound pressure level above that frequency.

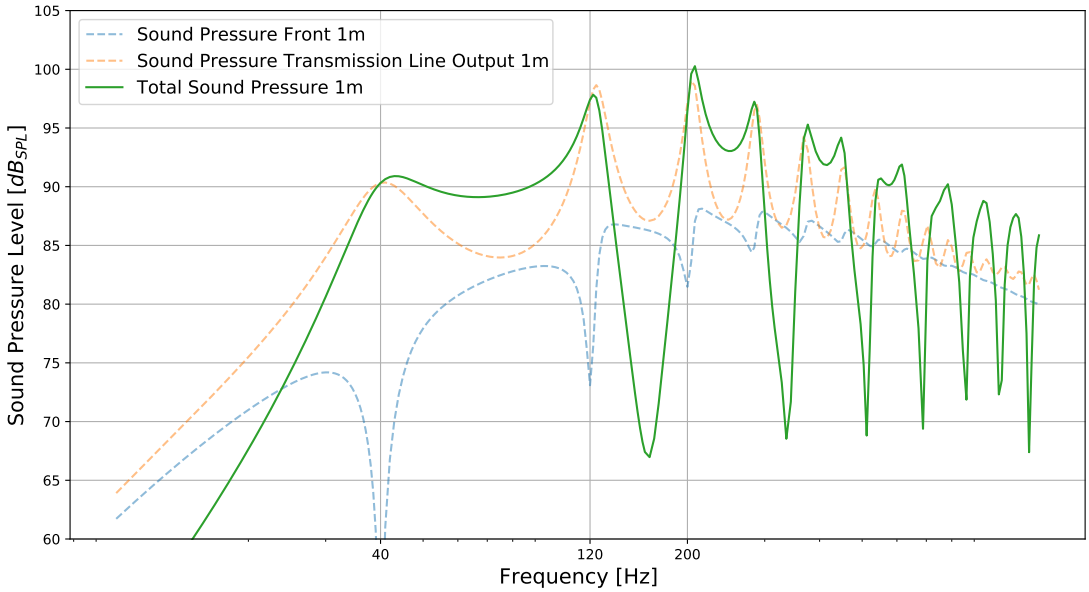

Figure 5.5: Sound Pressure Level of the Transmission Line at One Meter

5.1.5 Sound Pressure Modes

Figure 5.6 shows the absolute value of sound pressure at every point x in the line for the first two resonant frequencies visible in figure 5.4 being 40 Hz and 123 Hz, as well as resonant frequencies calculated with equation 5.1 being 43 Hz and 129 Hz.

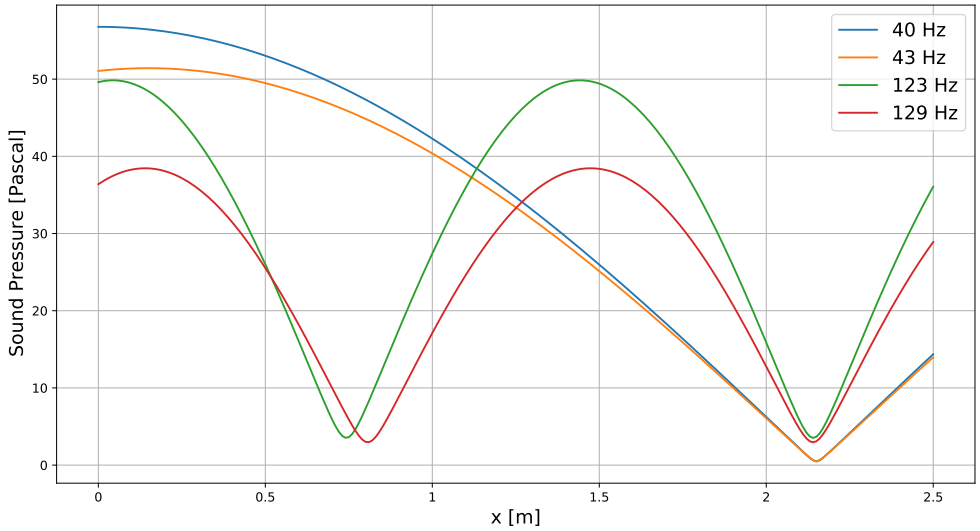

Figure 5.6: Sound Pressure Modes

Note that the quarter wave frequencies calculated with equation 5.1 have standing waves slightly shifted towards the open end of the line compared to quarter wave resonances found in figure 5.4, as positive interference does not happen exactly at $x = 0$ due to the phase shift for the reflected sound pressure wave at the open end of the line being less than 180°.

5.2 Simulation of a Paraflex System

Figure 5.7 shows the configuration of the "Paraflex" system for the second test case. Again, the output of the system is assumed to sit in an infinite baffle, therefore acoustic impedance at this point must be equal to acoustic impedance given in equation 4.1.

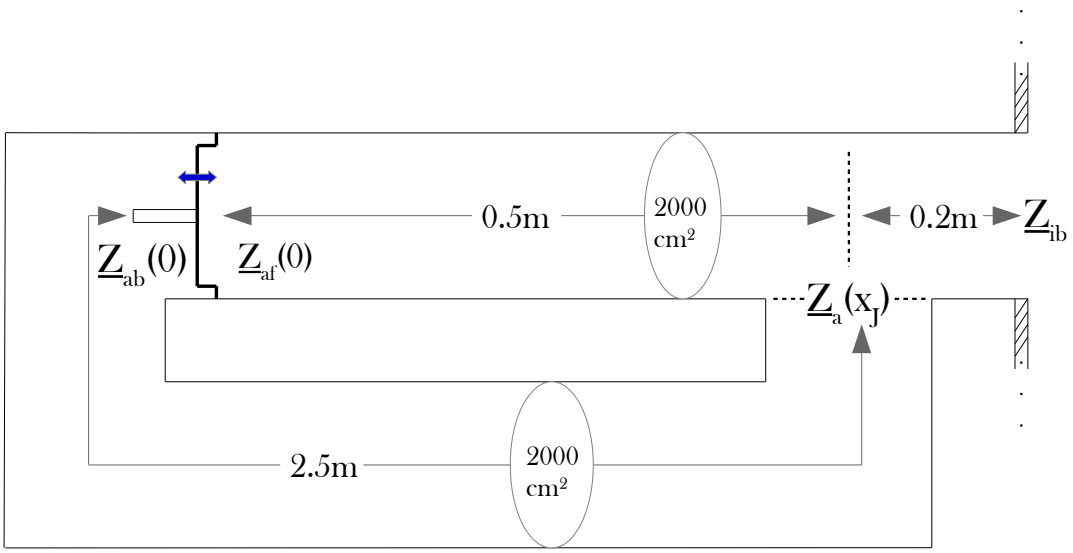

Figure 5.7: Simulated Paraflex System

The HTR is of total length 0.7 m, composed out of two transmission line segments with length 0.5 m and 0.2 m and the same cross sectional area of 2000 cm^2 ($d = 50$ cm), while the LTR consists of one transmission line segment of length 2.5 m and 2000 cm^2 cross sectional area. As mentioned in chapter 4.1, the segment of length 0.2 m corresponds to the segment of the HTR shared with the LTR, therefore, total effective length of the LTR is equal to 2.7 m. As will be shown in chapter 5.2.1 the fundamental resonant frequency of the LTR indeed corresponds to a length of 2.7 m, however, this will need further confirmation by measurements as the simulated model assumes the shared segment to be effective for the LTR.

The system is powered by a loudspeaker driver with the following parameters:

$S_d = 855\ \mathrm{cm}^2$ ($d = 33$ cm)
$Bl = 28.4\ \frac{N}{A}$
$M_{md} = 161\ \mathrm{g}$
$C_{ms} = 133\ \frac{\mu\mathrm{m}}{N}$
$R_{ms} = 8.4\ \frac{\mathrm{kg}}{\mathrm{s}}$
$R_s = 5.1\ \Omega$
$L_s = 1.9\ mH$

Again, input peak voltage of the voltage source $\underline{U}_g$ is equal to one volt.

5.2.1 Acoustic Input Impedance

Figure 5.8 shows the absolute value of the acoustic input impedance to the HTR and LTR at the front and back of the loudspeaker driver respectively, computed with equation 4.3 and 4.6.

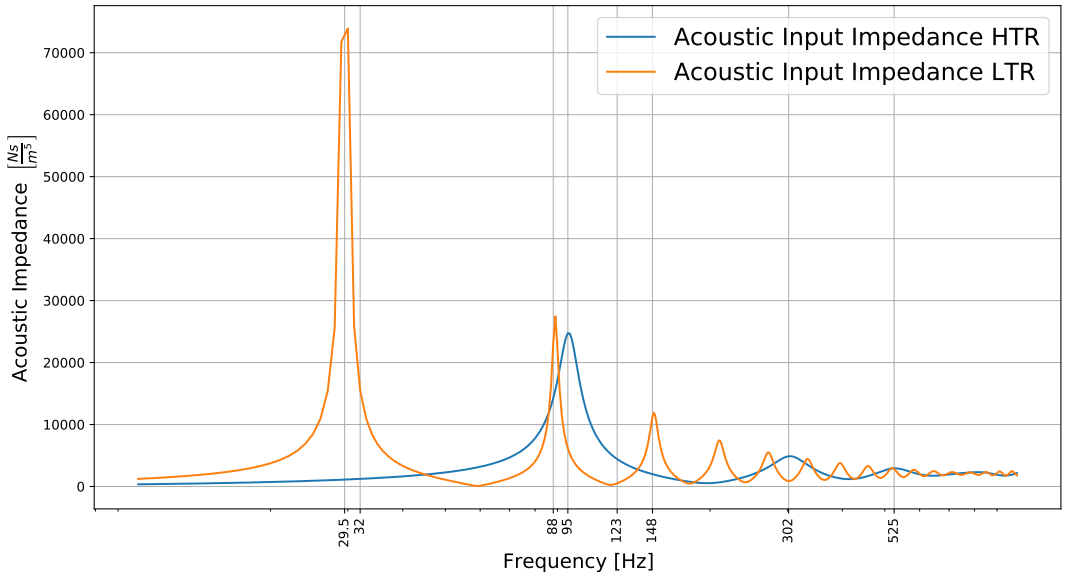

Figure 5.8: Acoustic Input Impedances of the Paraflex System

As both transmission line segments of the HTR are of the same cross sectional area, they can be seen as one long resonator of total length $L_{HTR} = 0.7\,\text{m}$. This results in fundamental resonance frequency of about 123 Hz if calculated with equation 5.1. As highlighted in figure 5.8, this is shifted down to 95 Hz due to a respective phase shift happening at the open end of the line as discussed in chapter 5.1.1, effectively increasing the length of the transmission line segment. Also, the second and third resonance of the HTR being 302 Hz and 525 Hz are highlighted in figure 5.8.
For the LTR, total length from source to the open end of the line is equal to 2.7 m, which corresponds to a fundamental resonance sitting at about 32 Hz. As highlighted in figure 5.8, this again is shifted down to 29.5 Hz, which is equal to a quarter wavelength of about 2.9 m. This again corresponds to the increase of effective length of the LTR from source to the open end of the system due to a phase shift smaller than 180° for the reflected wave. With fundamental resonance of the LTR corresponding to the total length from source to mouth of 2.7 m, we can conclude, that the shared line segment of 0.2 m length adds up to the total length of the LTR, consequently lowering fundamental resonance frequency as mentioned in chapter 1. Again, the second and third resonance of the LTR being 88 Hz and 148 Hz are highlighted as well.

5.2.2 Electric Input Impedance

Figure 5.9 shows the absolute value of the electric input impedance of the system computed with equation 4.9, with $\underline{Z}_{TL1e}$ being the electric equivalent of the acoustic input impedance to the HTR and $\underline{Z}_{TL2e}$ being the electric equivalent of the acoustic input impedance to the LTR. Again, electric equivalents of the total acoustic impedance faced by the membrane as well as the mechanic impedance of the loudspeaker driver are shown as well.
Like in chapter 5.1.2, peaks in total electric input impedance correspond to high driver motion and minimum impedance corresponds to minimal driver motion at resonant frequencies of the transmission lines. Therefore we get minimum electric input impedance at resonant frequencies

of the LTR being 29.5 Hz, 88 Hz and 148 Hz as well as resonant frequencies of the HTR being 95 Hz, 302 Hz and 525 Hz, although not being significant for the second and third resonance of the HTR.

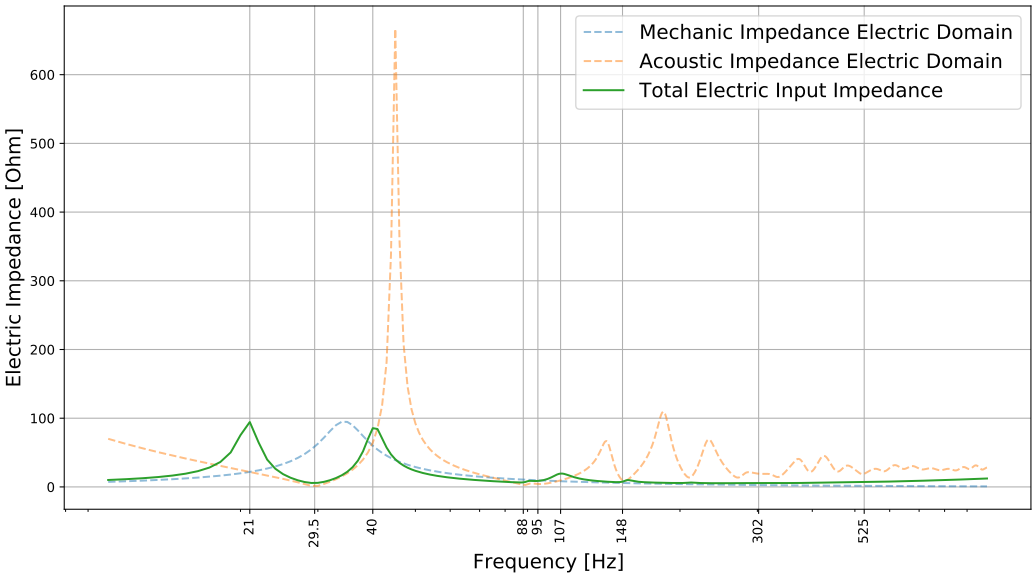

Figure 5.9: Electric Input Impedance of the Paraflex System

5.2.3 Sound Pressure at x_J

Figure 5.10 shows the absolute value of the sound pressure of the HTR $[p_{L1}(x_J)]$ and LTR $[p_{L2}(x_J)]$ at x_J, computed with equations 4.18 and 4.19, as well as total sound pressure $p(x_J)$ at x_J given by equation 4.20.

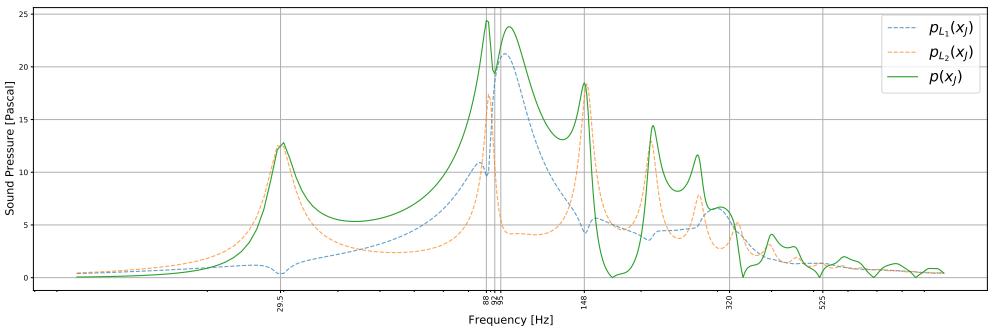

Figure 5.10: Sound Pressure at x_J

Peaks in sound pressure of the HTR and LTR can be seen at about the resonant frequencies found in chapter 5.2.1, again including a small shift that will need further investigation. Complex addition of these sound pressures leads to total sound pressure $p(x_J)$ at x_J. If we have a look at the phase diagram of the respective sound pressures at x_J in figure 5.11, we can see phase coherence and therefore positive interference of $p_{L1}(x_J)$ and $p_{L2}(x_J)$ for most of the frequencies between 29.5 Hz and 148 Hz. Only at about 92 Hz, some deviation in phase appears, therefore there is some amount of cancellation occurring in the total response as can be seen in figure 5.10.

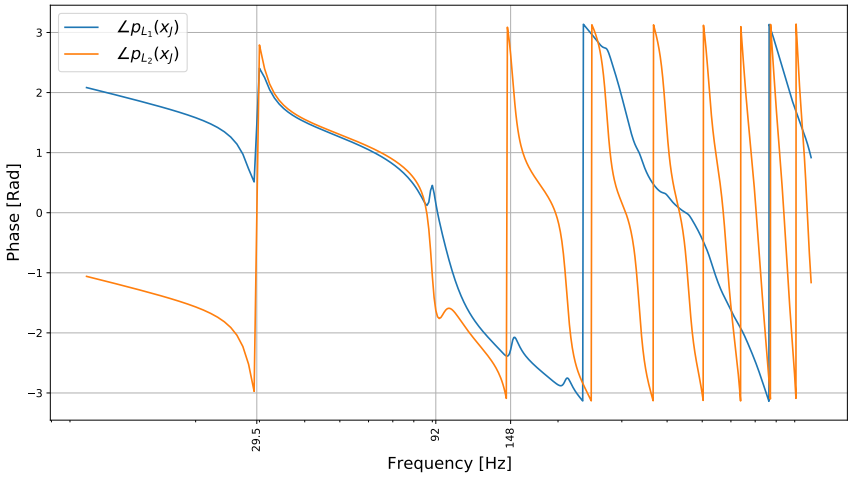

Figure 5.11: Phase at x_J

At frequencies above 148 Hz, phase relation between sound pressure of the HTR and LTR leads to alternating positive addition and negative cancellation due to larger deviation in phase. Therefore, the working bandwidth of a "Paraflex" loudspeaker system is limited to frequencies of about the third resonant frequency of the LTR.
Figure 5.10 also shows minimum sound pressure for the HTR at resonant frequencies of the LTR, the first three being 29.5 Hz, 88 Hz and 148 Hz. As can be seen in figure 5.9, electric input impedance is at minimum for these frequencies corresponding to minimal driver motion at these points of interest. As the HTR is not at resonance at these frequencies, minimal driver motion leads to minimal sound pressure generated, resulting in the mentioned dips in response. For resonant frequencies of the HTR though, there does not seem to be significant influence on sound pressure generated by the LTR.

5.2.4 Output Sound Pressure

Output sound pressure of the system can be calculated with equation 4.22. This is shown in figure 5.12.

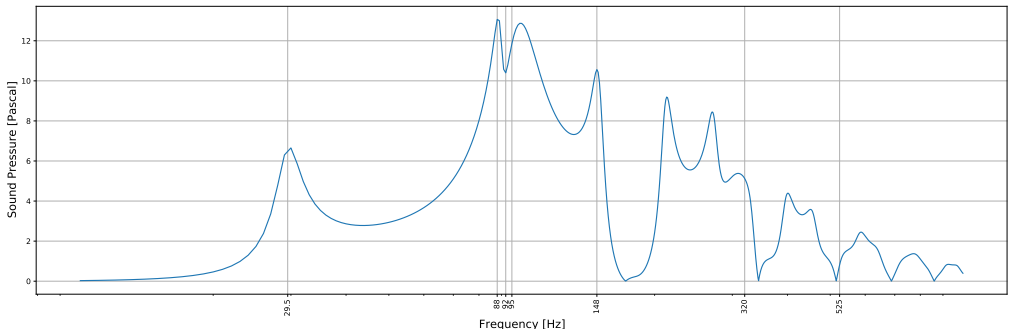

Figure 5.12: Output Sound Pressure

As one can see, the output sound pressure is very similiar to the one obtained at $x = x_J$ shown in figure 5.10 and can further be used to compute sound pressure response at one meter distance using equation 4.25.

5.2.5 Sound Pressure Level at One Meter

Figure 5.13 shows the sound pressure level of the "Paraflex" system at one meter distance, computed with equation 4.25 and 4.26.

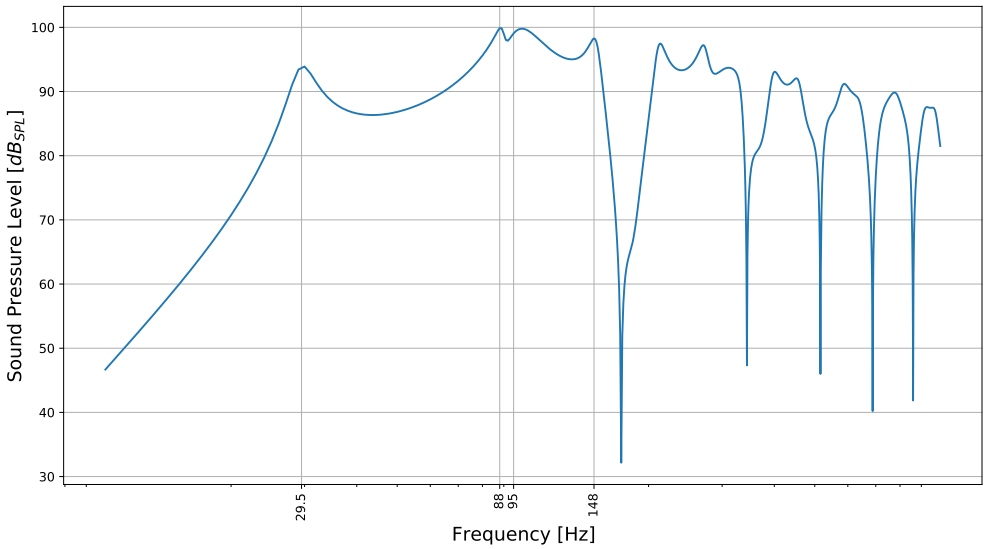

Figure 5.13: Sound Pressure Level at One Meter

Again, distinct peaks are visible at the resonant frequencies found in chapter 5.2.1. Compared to the frequency response of the simulated transmission line system shown in figure 5.5, the working bandwidth of the "Paraflex" system is increased as two distinct resonators tuned to different resonant frequencies are providing sound pressure output, covering a wider range from the fundamental resonance of the LTR at 29.5 Hz up to its third resonance at 148 Hz. For a transmission line loudspeaker system, the working range is limited to frequencies between the first and second line resonance, as there is a big dip in frequency response after the second resonant frequency, as can be seen in figure 5.5. Crucially for the "Paraflex" loudspeaker system shown in figure 5.7, fundamental resonance of the HTR at 95 Hz sits at about the second resonant frequency of the LTR at 88 Hz, providing sound pressure output for the overall system in this range as can be seen in figure 5.10, therefore increasing overall bandwidth of the system due to good phase alignment of the resonators in this region.
Overall, the frequency response of the simulated "Paraflex" loudspeaker system has major sound pressure level differences of more than 10 dB_{SPL} in its working range, which does not make it suitable for real life usage. However, the particular setup of figure 5.7 is not representative of existing "Paraflex" loudspeaker cabinets, as it is only a simplified configuration for demonstration purposes on how this kind of loudspeaker works. Different length for the HTR and LTR, changes in cross sectional area as well as different driver parameters all influence the final response and efficiency of the respective cabinet, therefore the development of a working design is a complex process which exceeds the limits of this work. Also, digital signal processing will be necessary to flat out the overall frequency response, as is the case for most "Public Address" loudspeaker cabinets.

6 Conclusion and Future Work

6.1 Conclusion

In this work, a computational model to simulate system characteristics such as sound pressure level output, phase response or electric input impedance of a "Paraflex" loudspeaker enclosure was derived. The model is based on electric circuit analysis of the electric analogous circuit, containing only lumped elements describing the respective loudspeaker system. As "Paraflex" loudspeaker enclosures are based on the concept of acoustic quarter wave resonators, computations for the distributed elements of acoustic transmission lines describing such resonators had to be derived to be able to obtain acoustic input impedances to the lines faced by the loudspeaker membrane, as was done in chapter 3. With acoustic input impedances at hand, it was possible to transform the electromechanoacoustic analogous circuit of the system containing lumped elements only to the electric domain. Consequently, electric circuit analysis was performed to obtain crucial system characteristics such as electric input impedance or input volume velocities to the resonators as done in chapter 4.3.1 and 4.3.2. Eventually, it was possible to compute system output sound pressure by again making use of equations derived in chapter 3.2.3.
As the concept of "Paraflex" loudspeaker systems is based on acoustic transmission lines, to get a better understanding of how these enhance sound pressure output at low frequencies, a simple transmission line loudspeaker enclosure was simulated to analyse behavior of the quarter wave resonator over the frequency band of interest. With the graphs obtained, the necessary condition for frequencies to resonate in the lines given by equation 5.3 as well as relations between acoustic impedance faced by the membrane and mechanic impedance of the loudspeaker driver to form the total electric input impedance were found.
Subsequently, the more complex configuration of a "Paraflex" loudspeaker system was simulated and analysed. It was found that the behavior of this type of loudspeaker cabinet strongly correlates to the acoustic transmission line system analysed, albeit with more complex relations between sound pressure generated by the front and back side of the loudspeaker membrane. Eventually, comparison of the output sound pressure responses of both systems suggested wider bandwitdh for "Paraflex" loudspeaker cabinets, as two distinct resonators provide sound pressure output for different frequency ranges. Also, the transmission line segment shared by the HTR an LTR was found to be increasing total length for the LTR as mentioned in chapter 1, therefore lowering fundamental tuning. However, measurements will be necessary to further confirm this relation as the derived model assumes this to be true.

6.2 Future Work

As this work focused on deriving the computational model for "Paraflex" loudspeaker enclosures as well as analysing the behavior of the quarter wave resonators such a system is based on, relations between geometric dimensions of the enclosure such as cross sectional area or length of the resonators and the resulting system characteristics are yet to be examined. Also, effects of different driver parameters on system behavior and optimization of the enclosure regarding efficiency or low end response are yet to be discussed.

Furthermore, several assumptions were made for the discussed model to simplify relations derived describing the overall system. As every simplification adds potential errors in the simulation results compared to real life behavior, the following could be included in the future.

Acoustic Simplifications

For computations derived describing the acoustic transmission lines, neither bends in the line nor different shapes such as rectangular or triangular were discussed. As these most probably change wave propagation in the lines for certain frequency ranges, different shapes and bends should be taken into account to improve accuracy of the model.

Also, wave propagation in the transmission lines was assumed to be lossless for this work. Dissipation at the boundaries of the line or for acoustic waves propagating in air could therefore be discussed as well.

Finally, the system output was assumed to sit in an infinite baffle. For real world applications though, this hardly is the case so improved models for radiation impedance in more complex environments as well as consideration of diffraction on the baffle could be taken into account.

However, verification of the derived model by measuring acoustic characteristics of a real life "Paraflex" loudspeaker cabinet and comparing it to simulation results should be the main focus for future work on this topic. Also, the relation between geometry of the merge section and the resulting resonant frequencies for the HTR and LTR are of major interest as this enables designers to predict tuning of the resonators dependent on the geometric dimensions of the merge section more accurately. This will eventually lead to better understanding of the most important design parameters for "Paraflex" loudspeaker systems, making it a more convenient type of enclosure for designers to work with.